4.5 IMPLEMENTION OF WINDSAT DATA FROM NPOESS INTO 3DVAR FOR CANSAC REAL-TIME MM5 FORECASTING

Tesfamichael Ghidey*[1], Jülide Kahyaoglu-Koracin[1], Michael D. McAtee[2], and Timothy J. Brown[1]

[1]Desert Research Institute, Reno, Nevada

[2]AFWA/Aerospace Corp., Offutt AFB, Nebraska

1. INTRODUCTION

The Desert Research Institute Program for Climate, Ecosystem, and Fire Applications (CEFA) is the operational component of the California and Nevada Smoke and Air Committee (CANSAC) providing real-time meteorological, air quality, and fire danger forecasts for the CANSAC consortium and related scientific community to aid in decision making and atmospheric research particularly pertaining to fire weather, smoke transport and dispersion, and coastal studies. Given that the CANSAC products are used in California and Nevada for strategic planning and decision-making, the accuracy of the forecast products becomes a critical issue. In parallel to operational simulations with the Fifth Generation Penn Sate/NCAR Mesoscale Model (MM5) (Grell et al., 1994), a series of sensitivity studies in model physics options together with several data assimilation techniques are being conducted at CEFA in order to improve the overall numerical weather forecast results.

The purpose of this study is to examine the performance and the potential increase in accuracy of MM5 forecasts through the assimilation of WindSat data into the 3-Dimensional Variational Analysis (3DVAR) system over the Western US. The methods of integrating WindSat winds into MM5-3DVAR and preliminary results of its performance tests applied to a selected case in January 2005 are discussed in this paper.

2. OVERVIEW OF WINDSAT DATA

The main role of environmental satellites (geostationary and polar-orbiting) is to provide good quality observational data over large geographical regions where data are sparse or not available at all. Thus, satellite observations have become the primary source of data for oceanic regions. Recently, the Integrated Program Office (IPO) of the Department of Defense (DoD) Space Test Program (STP), the U.S. Navy and the National Polar-Orbiting Operational Environmental Satellite System (NPOESS) launched CORIOLIS in which its main payload is WindSat, for ocean surface wind vector measurements. WindSat is a multi-frequency polarimetric microwave radiometer developed by the Naval Research Laboratory (NRL) and IPO that is designed to primarily measure the ocean surface wind vector from space. WindSat winds are available at approximately 12.5x12.5 km^2 grid squares and are referenced at 10 m height. Such dense information of winds over the ocean and coastal regions is extremely important in understanding various weather phenomena as well as in improvement of short-term weather forecasting and coastal studies. In addition to wind vectors, the WindSat system provides secondary maritime data products such as column integrated cloud liquid water, column integrated precipitable water, and sea surface temperature (Lungu 2005). A full description of the WindSat system can be found in the WindSat user's manual (Lungu 2005).

3. 3DVAR SYSTEM

Courtier et al. (1994) have formulated a three dimensional variational algorithm in an incremental analysis. A similar algorithm has been developed for the MM5 3DVAR assimilation system by Barker et al. (2003; 2004). The configuration produces a model space based multivariate incremental analysis for pressure, wind, temperature, and relative humidity. The 3DVAR algorithm computes the analysis increment on an unstaggered "Arakawa-A" grid (Arakawa and Lamb 1977). After the incremental cost function minimization is performed in preconditioned control variables (such as stream function, velocity potential, unbalanced potential and humidity), the unstaggered analysis output increments are

*Corresponding author address: Tesfamichael Ghidey, Desert Research Institute/DAS, 2215 Raggio Parkway, Reno, NV 89512; email: Tesfamichael.Ghidey@dri.edu

converted to the "Arakawa B" grid of MM5. A balanced pressure is reproduced from the linearized mass-wind balance. The horizontal and vertical correlations functions are separated due to a well-designed background covariance matrix to project onto vertical modes, following Lorenc et al. (2000). Horizontal filter parameters are de-fined using the vertical eigenvector. The decomposition of empirical orthogonal functions (EOFs) of the statistical model forecast error covariances are used to find the vertical modes. The National Meteorological Center (NMC) method is used to estimate the climatological background error covariances by employing the statistical differences between the 24- and 12-h forecasts (Parrish and Derber 1992).

In this study, the global background error covariance (domain size of 101-X181X21 with 210 km grid distance) prepared by the NCAR group was used. After projection onto the vertical modes, three-dimensional meteorological variables are normalized by the square root of the variance (eigenvalue) of the relevant vertical mode. Following normalization, these normalized fields are brought into a series of recursive filters, which create the smoothing effect of a convolution with a covariance matrix. Under the application of this recursive filter, the horizontal model forecast error correlations are homogenous and isotropic.

4. METHODOLOGY

The present study contained a short-range forecast for a cold-starting mode of MM5 3DVAR on 3 January 2005 at 1200 UTC. This period is chosen because it has large maritime observational wind vector dataset records for use as initial analysis time into 3DVAR.

MM5 simulations optimized by 3DVAR output were carried out to achieve the following goals:

- To modify the observation pre-processor to ingest WindSat data including the assignment of observation errors specific to WindSat (Lungu 2005).
- To clone an existing 3DVAR wind observation operator and its related files (QuikScat operator) so that it can be used for WindSat data.
- To Run and verify the performance of MM5 prediction with and without WindSat data.

MM5 was used with a Lambert Conformal map projection centered at 38.0ºN latitude, 121.0ºW longitude. Three nested horizontal domains (grid spacing of 36, 12, and 4 km) are used (Fig. 1), with 93 x 93, 154 x 154, and 274 x 274 grid-points, respectively. Two-way nesting was also used in which information is fed to the next outer domain at each time step with no feedback to the inner domains. Other options selected for all domains include: Dudhia (1993) radiation to account for long- and short-wave cloud-interactions; Dudhia (1993) explicit simple-ice moisture, and ETA Planetary Boundary Layer (PBL) scheme (Janjic 1994) with turbulent kinetic energy (TKE). The Grell et al. (1994) non-shallow cumulus convection (no equilibrium assumed between cloud-strength and sub-grid PBL forcing) was used only in the outer two domains. ETA model (40 km grid-resolution) provided "first guess" initial and boundary conditions at 12-h intervals. A radiative vertical-motion upper-boundary condition (recommended for grid lengths < 50 km) was used to reduce energy-reflection, thus preventing spurious noise or energy build-up over significant topographic features. The five-layer soil-model option of Dudhia (1996) was also used.

Each simulation (with and without 3DVAR initialization) started at 0500 PDT (1200 UTC) on 3 January 2005 and ran for 72 hours. The Read-Interpolate-Plot (RIP) graphical package (Stoelinga 1991) was used to display MM5 output after 12-hour spin-up period. Both MM5 outputs with and without 3DVAR initialization were qualitatively (using Domain 1 or coarser domain) compared to each other using lowest model half-sigma level (~10m) temperature fields, and horizontal wind vectors. In the next section qualitative surface results are discussed.

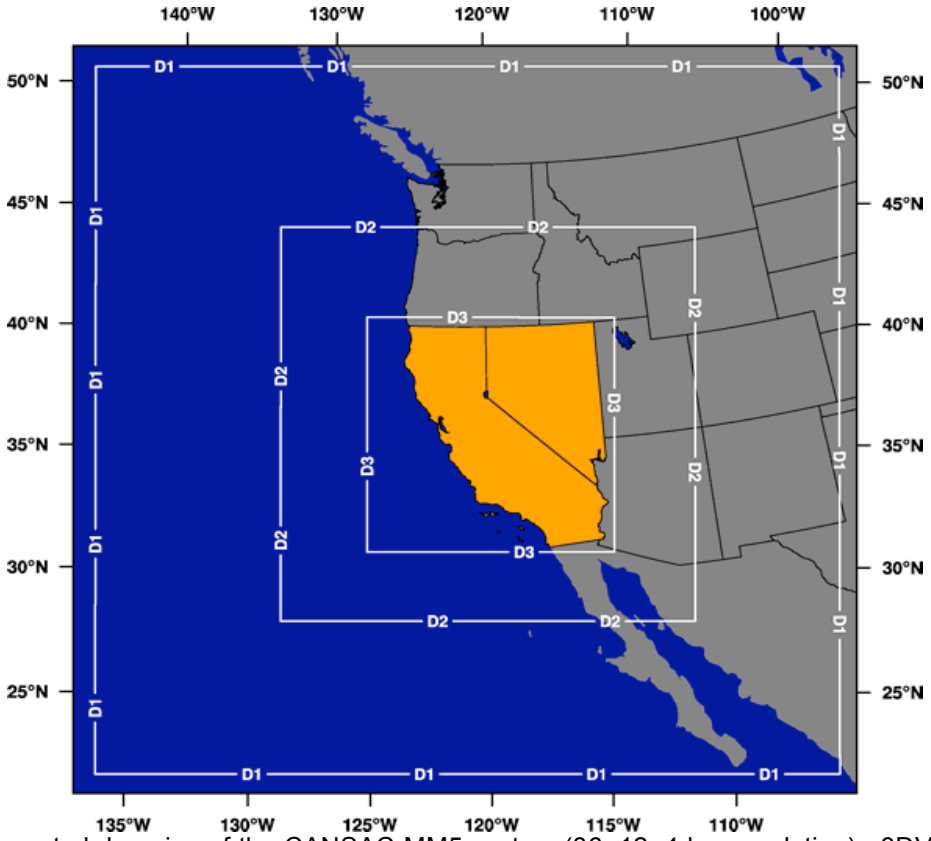

Figure 1. Three nested domains of the CANSAC MM5 system (36, 12, 4 km resolution). 3DVAR is used in all nested domains to initialize MM5. Coordinates are geographical latitudes and longitudes.

5. RESULTS

Upon implementation of WindSat data into the 3DVAR system, the 3DVAR code was run to produce diagnostic analysis for use in MM5 as initial conditions, and diagnostic analysis increments to evaluate the incremental cost function minimization. Diagnostic analysis increments of surface pressure, u- and v-component wind were plotted for the coarser domain to show their increment values. Pressure increments were mostly positive over most of the coarser domain (36 km) with a central high value of 1.06 hPa (Fig. 2, solid contours) centered over the offshore area of Baja of California, and a central low -0.402 hPa centered over the eastern central Pacific Ocean (Fig. 2, dashed contours). Increments of u-component winds showed that most of Domain 1 was negatively incremented with a central value of -2.05 m s^{-1} (Fig.3, dashed contours) centered over offshore of southern California, and positively incremented over areas of far west part of the Pacific Ocean and over inland area of north of California and Nevada with central highs of 1.59 and 1.52 m s^{-1} centered both over the southwest corner and northwest part of the domain (Fig. 3, solid contours), respectively. Similarly, the incremental values of the v-component were also mostly negative over the domain with two central values of -2.28 and -2.46 m s^{-1} (Fig. 4, dashed contours) both centered over the north and south Pacific Ocean of the domain, and some inland positive increment was also located over Four Corner States and Mexico with central values of about 0.6 and 1.06 m s^{-1} (Fig. 4, solid contours), respectively. These diagnostic analyses increments of the meteorological fields showed the proper performance of 3DVAR code with the newly assimilated WindSat data.

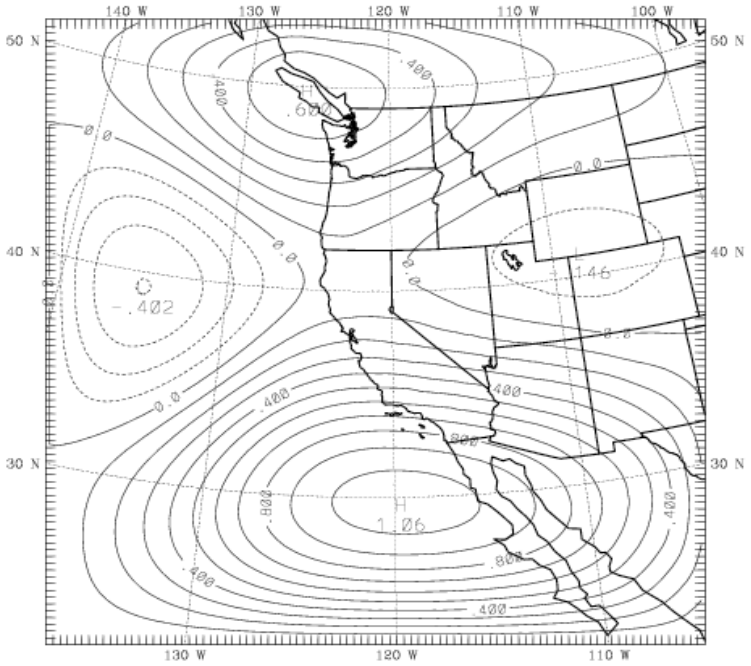

Figure 2. Diagnostic analysis increment of pressure (hPa) at the surface on Domain 1 (36 km) at the initial analysis time of 1200 UTC on 3 January 2005. Note that solid contours are positive and dashed contours are negative analysis increments. Coordinates are geographical latitudes and longitudes, and contour interval is 0.1 hPa.

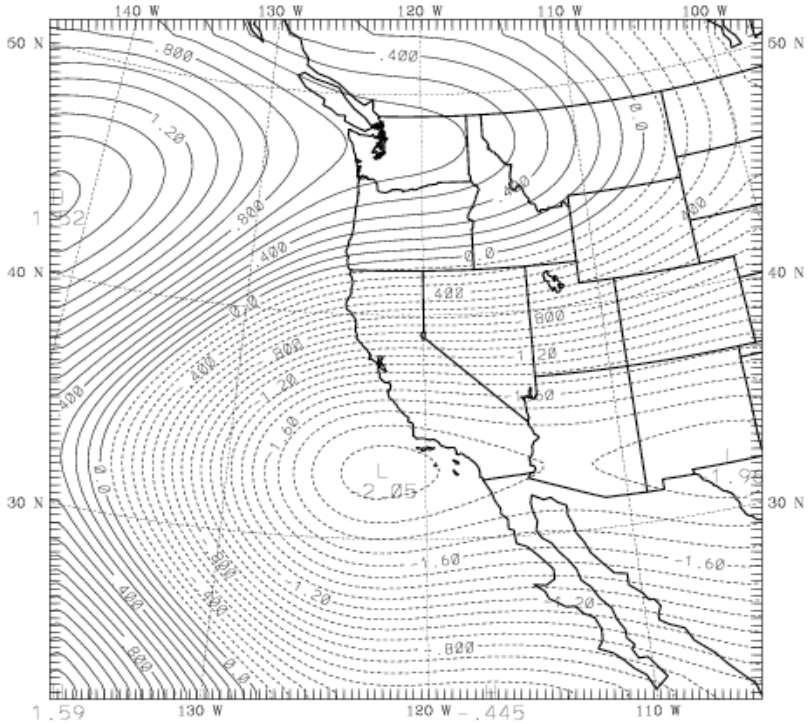

Figure 3. Diagnostic analysis increment of u-component wind (m s^{-1}) at the surface on Domain 1 (36 km) at the initial analysis time of 1200 UTC on 3 January 2005. Note that solid contours are positive and dashed contours are negative analysis increments. Coordinates are geographical latitudes and longitudes, and contour interval is 0.1 m s^{-1}.

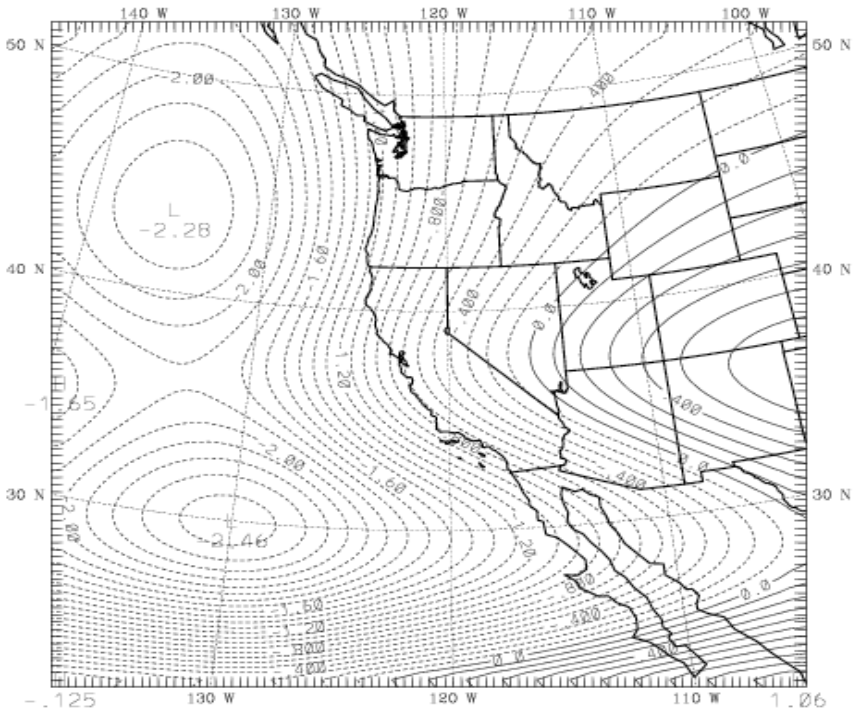

Figure 4. Diagnostic analysis increment of v-component wind (m s^{-1}) at the surface on Domain 1 (36 km) at the initial analysis time of 1200 UTC on 3 January 2005. Note that solid contours are positive and dashed contours are negative analysis increments. Coordinates are geographical latitudes and longitudes, and contour interval is 0.1 m s^{-1}.

Two MM5 simulations were carried out to evaluate the impact of the 3DVAR system on the mesoscale meteorological fields. First, MM5 was initialized with ETA large scale first guess input without any observational preprocessing, while the second MM5 run was done after the initial and boundary conditions were prepared by 3DVAR system using WindSat maritime data. Here, surface comparisons are given special attention to evaluate the impact of WindSat dataset.

Surface horizontal wind vectors (~10 m) 12 h into the forecast period (4 January 2005) of Domain 1 (coarser domain) were taken for qualitative comparison between model output with (here-after referred to as 3DVAR-MM5) and without (hereafter referred to as ETA-MM5) 3DVAR initialization. A synoptic weak low mean sea level pressure was located in the eastern Pacific Ocean west of Monterey Bay in the ETA-MM5 output. Synoptic wind flows were mostly northerly in the Pacific Ocean, while winds inlands were weak and following the offshore weak cyclonic flow, and warm temperatures at southern part of the domain were forecasted decreasing with upper latitudes as we go northward (Fig. 5). In the 3DVAR-MM5 forecast, the offshore central low-pressure system had slightly weakened when compared with ETA-MM5 output. Wind speeds were almost similar, while wind flow was more organized over the Pacific Ocean with a slight decrease in temperatures over most of the domain in the 3DVAR-MM5 result (Fig. 6). Twenty-four hours later (5 January), the low had further moved inland northeastward centered over northern Utah in both ETA-MM5 (Fig. 7) and 3D-VAR-MM5 (Fig. 8) outputs.

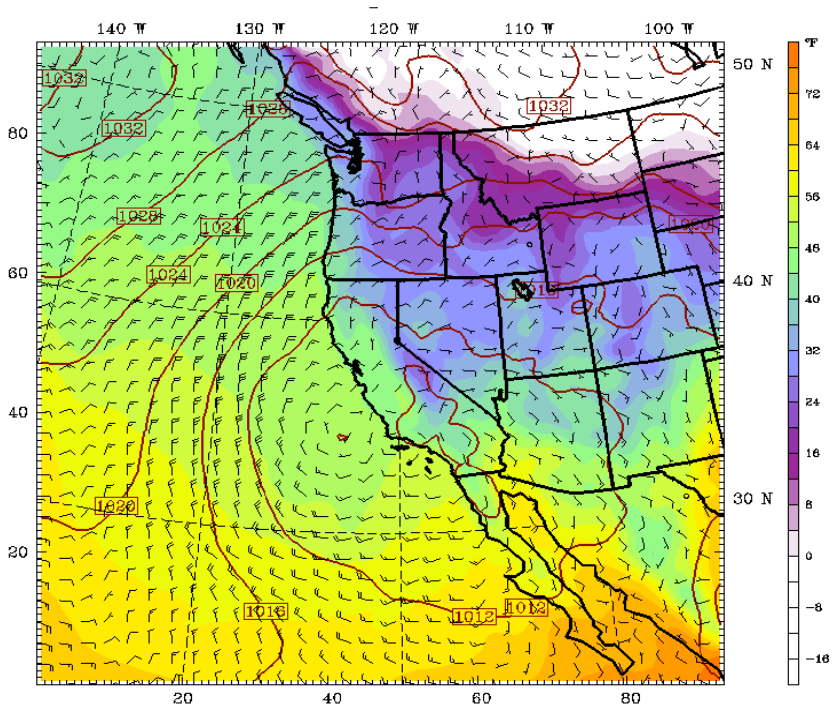

Figure 5. Domain 1 (36 km grid distance) MM5 output initialized with only ETA first guess depicting sea level pressure, surface (~10 m) horizontal wind vectors, and temperature on 4 January 2005 at 0000 UTC (3 January 2005 at 1600 PST) after 12 h spin-up. Full barb = 10 mi hr^{-1} (= ~4.5 m s^{-1}).

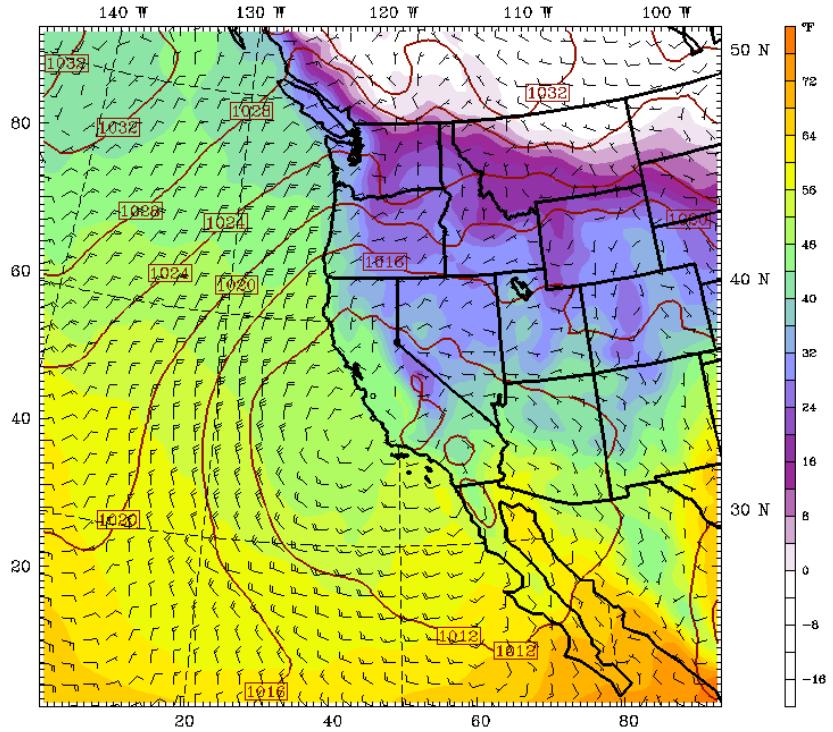

Figure 6. Domain 1 (36 km) MM5 output initialized with 3DVAR system depicting sea level pressure, surface (~10 m) horizontal wind vectors, and temperature on 4 January 2005 at 0000 UTC (3 January 2005 at 1600 PST) after 12 h spin-up. Full barb = 10 mi hr^{-1} (= ~4.5 m s^{-1}).

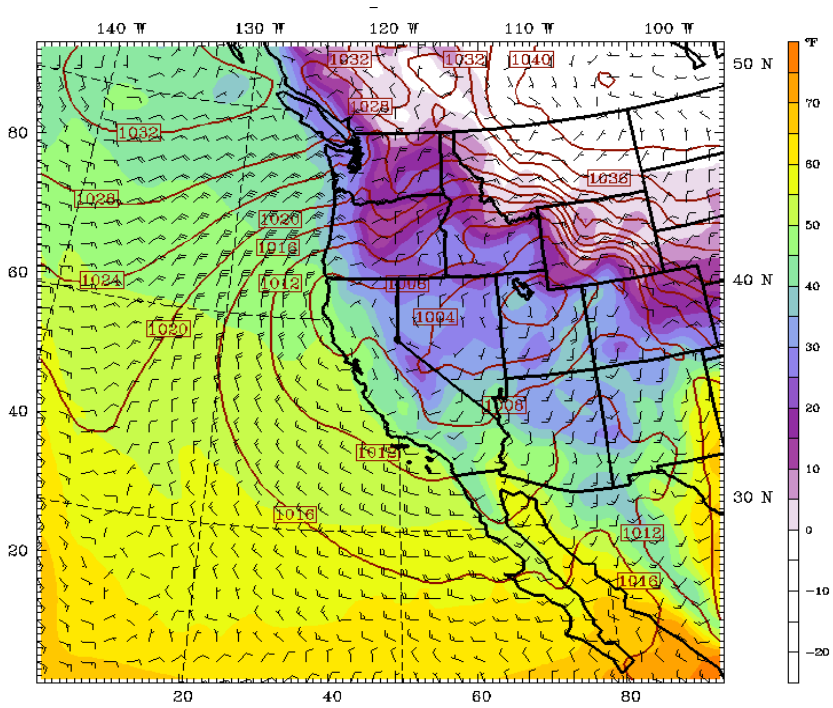

Figure 7. Domain 1 (36 km) MM5 output initialized with only ETA first guess depicting sea level pressure, surface (~10 m) horizontal wind vectors, and temperature on 5 January 2005 at 0000 UTC (4 January 2005 at 1600 PST) 36 h after model initialization. Full barb = 10 mi hr^{-1} (= ~4.5 m s^{-1}).

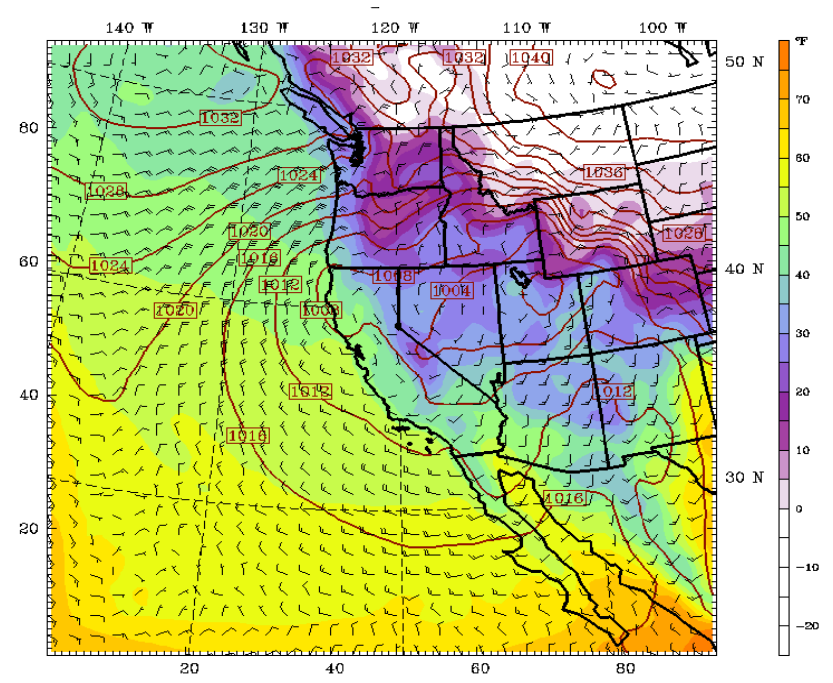

Figure 8. Domain 1 (36 km) MM5 output initialized with 3DVAR system depicting sea level pressure, surface (~10 m) horizontal wind vectors, and temperature on 5 January 2005 at 0000 UTC (4 January 2005 at 1600 PST) 36 h after model initialization. Full barb = 10 mi hr^{-1} (= ~4.5 m s^{-1}).

As the coarser domain has relatively low-resolution from the other nested domains, qualitative comparisons is also important over higher resolution (finest domain) to closely verify the impact of 3DVAR. Accordingly, surface horizontal wind vector results on 4 January 2005 0000 UTC of Domain 3 (4 km) were taken to compare 3DVAR-MM5 against ETA-MM5. The synoptic weak low mean sea level pressure was also located in the eastern Pacific Ocean west of Monterey Bay slightly moved south from the coarser domain in both cases. Comparing ETA-MM5 (Fig. 9) and 3dVAR-MM5 (Fig. 10), the 3DVAR-MM5 reproduced the low more distinctly organized than the ETA-MM5 output. Moreover, offshore synoptic wind flows were stronger near coastal San Francisco Bay Area (SFBA) and weaker over coast of Monterey Bay in the 3DVAR-MM5 than the ETA-MM5 result. Thirty-six hours into the forecast (on 5 January at 000 UTC), the low, as in the coarser domain, had further moved inland to northeastward now centered over central Nevada, but further weakened in both ETA-MM5 and 3DVAR-MM5 outputs. Weaker wind flows were however forecasted over most of the domain in 3DVAR-MM5 (Fig. 12) than ETA-MM5 results (Fig. 11).

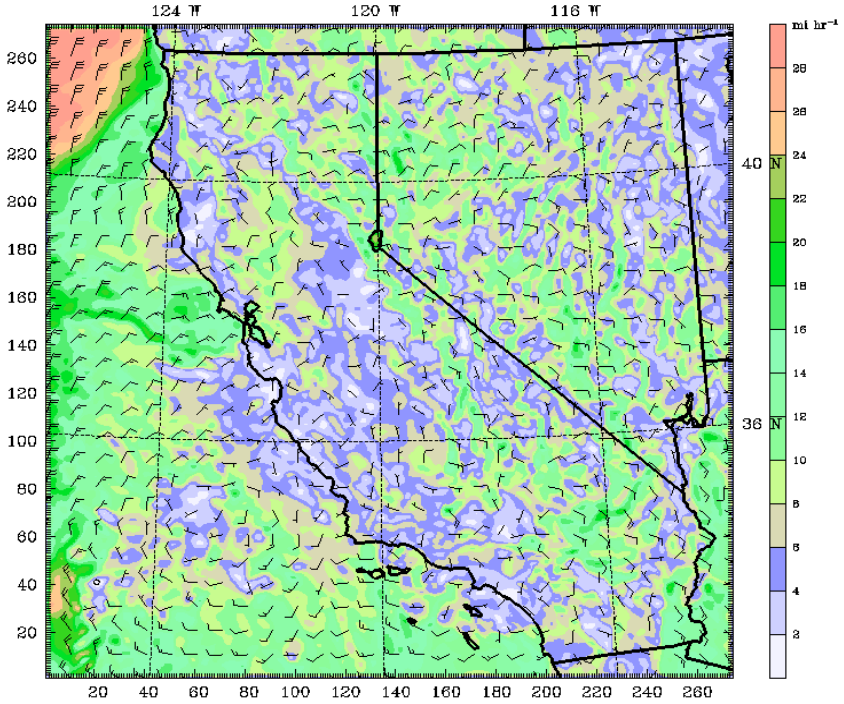

Figure 9. Domain 3 (4 km grid distance) MM5 output initialized with only ETA first guess depicting surface (~10 m) horizontal wind vectors (barbs) and horizontal wind speed (color shading) on 4 January 2005 at 0000 UTC (3 January 2005 at 1600 PST) after 12 h spin-up. Full barb = 10 mi hr^{-1} (= ~4.5 m s^{-1}).

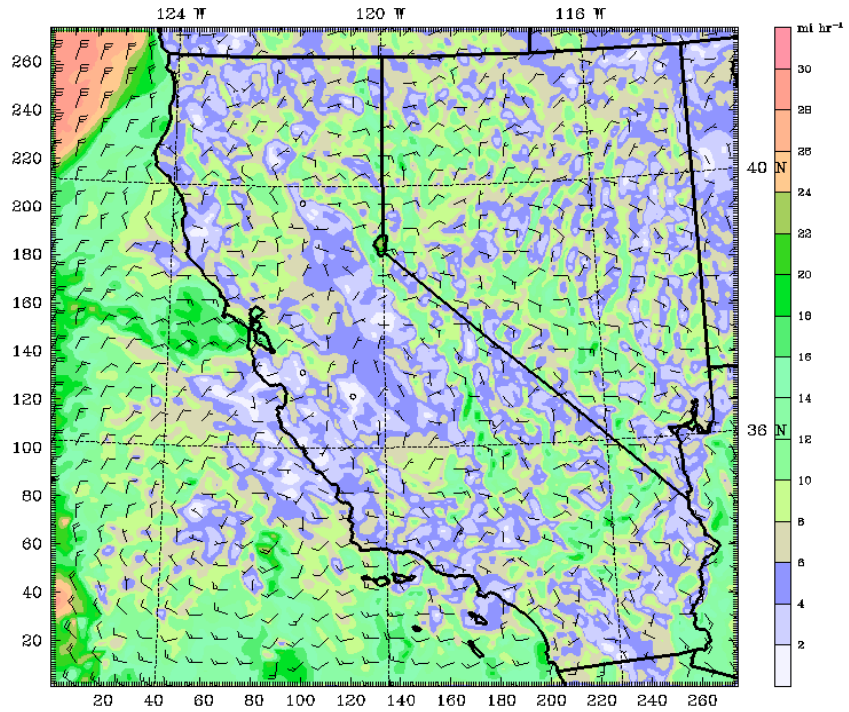

Figure 10. Domain 3 (4 km) MM5 output initialized with 3DVAR system depicting surface (~10 m) horizontal wind vectors (barbs) and horizontal wind speed (color shading) on 4 January 2005 at 0000 UTC (3 January 2005 at 1600 PST) after 12 h spin-up. Full barb = 10 mi hr^{-1} (= ~4.5 m s^{-1}).

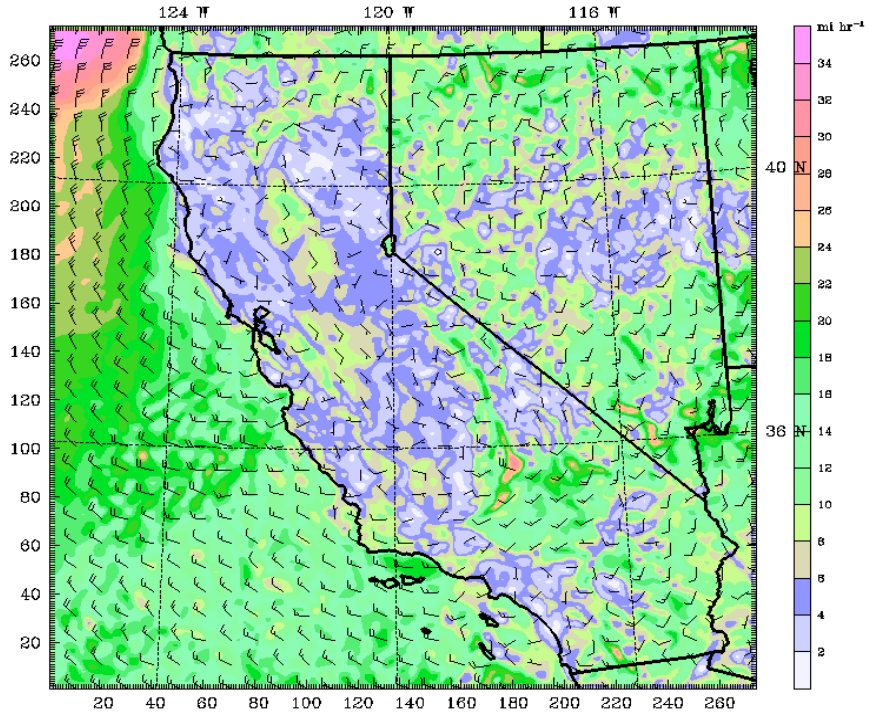

Figure 11. Domain 3 (4 km) MM5 output initialized with only ETA first guess depicting surface (~10 m) horizontal wind vectors (barbs) and horizontal wind speed (color shading) on 5 January 2005 at 0000 UTC (4 January 2005 at 1600 PST) 36 h after model initialization. Full barb = 10 mi hr^{-1} (= ~4.5 m s^{-1}).

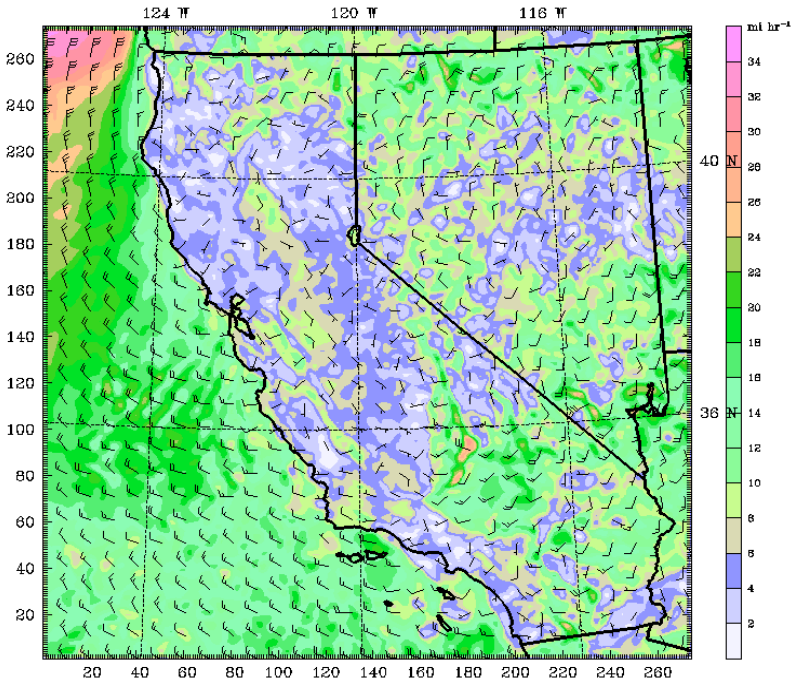

Figure 12. Domain 3 (4 km) MM5 output initialized with 3DVAR system depicting surface (~10 m) horizontal wind vectors (barbs) and horizontal wind speed (color shading) on 5 January 2005 at 0000 UTC (4 January 2005 at 1600 PST) 36 h after model initialization. Coordinates are horizontal domain grid points. Full barb = 10 mi hr^{-1} (= ~4.5 m s^{-1}).

A closer look into the finest domain allows for a more distinctive comparison between the cases because more informative grid points are revealed when zoomed in, that were skipped in the lower resolution domains. The 4 km domain was further zoomed in around most of western and central Nevada that includes Lake Tahoe and part of Sierra Nevada Mountains to help distinguish the qualitative differences between run cases. The ETA-MM5 (Fig. 13) result on 4 January 2005 at 0000 UTC showed stronger north-easterly winds north of Reno (near Lake Tahoe) than the 3DVAR-MM5 (Fig. 14). Winds were also stronger over the southern Sierras in the ETA-MM5 output than in the 3DVAR-MM5 case, while the flows were slightly stronger at the passage of the eastern side of the Sierras towards Lake Tahoe in the 3DVAR-MM5 output than the ETA-MM5 result. Twenty-four hours later on 5 January at 0000 UTC the upslope flows were overcome by the northwesterly strong synoptic flow in both cases. The wind flows in the ETA-MM5 output (Fig. 15) still showed stronger north-northwesterly direction than the 3DVAR-MM5 (Fig. 16) output over most of the region, maintaining the influence of initial conditions of 3DVAR system.

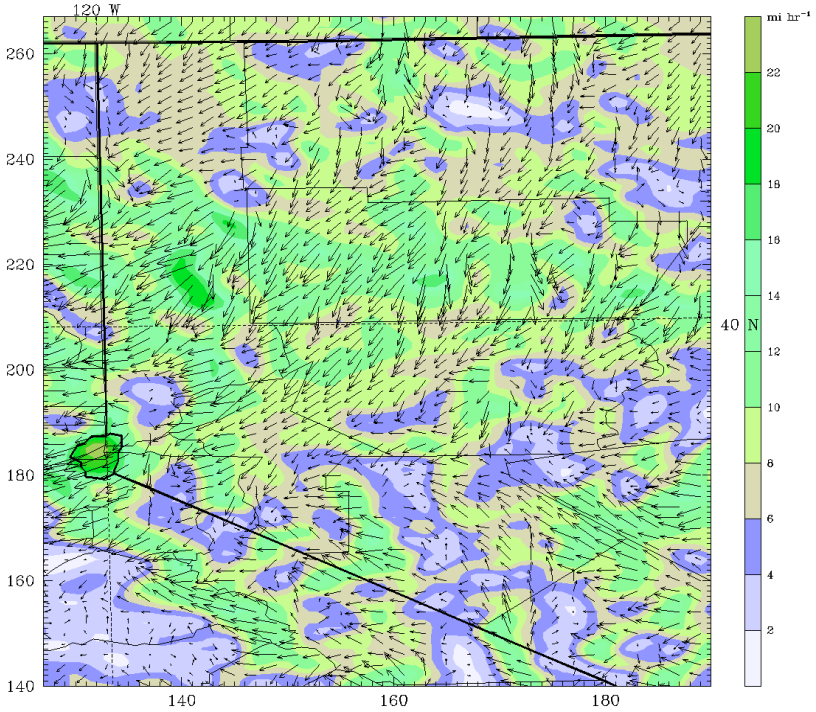

Figure 13. Zoom-in part of Domain 3 (4 km) MM5 output initialized with only ETA first guess depicting surface (~10 m) horizontal wind vectors (vectors) and horizontal wind speed (color shading) on 4 January 2005 at 0000 UTC (3 January 2005 at 1600 PST) after 12 h spin-up. Coordinates are horizontal domain grid points. Full barb = 10 mi hr^{-1} (= ~4.5 m s^{-1}) .

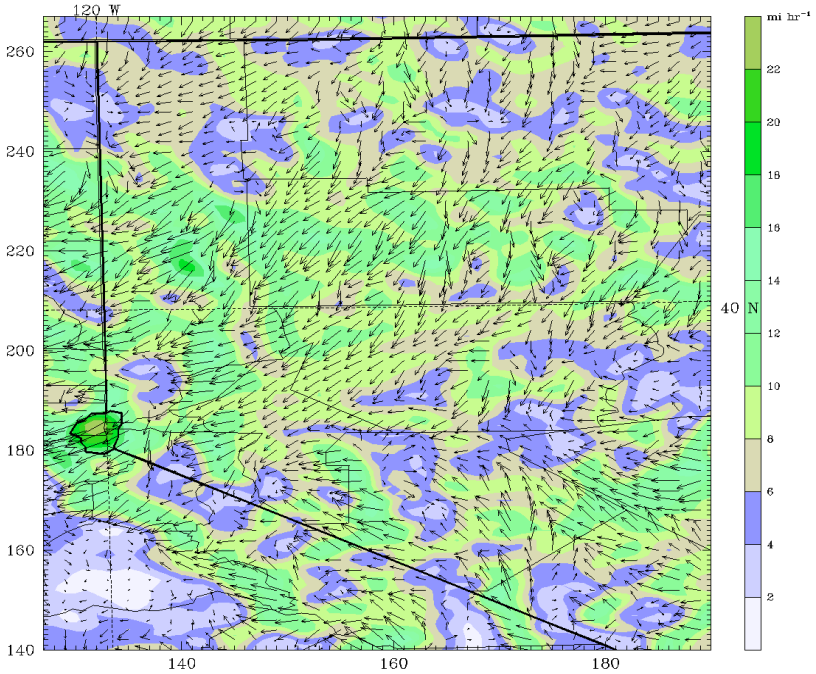

Figure 14. Zoom-in part of Domain 3 (4 km) MM5 output initialized with 3DVAR system depicting surface (~10 m) horizontal wind vectors (vectors) and horizontal wind speed (color shading) on 4 January 2005 at 0000 UTC (3 January 2005 at 1600 PST) after 12 h spin-up. Coordinates are horizontal domain grid points. Full barb = 10 mi hr^{-1} (= ~4.5 m s^{-1}).

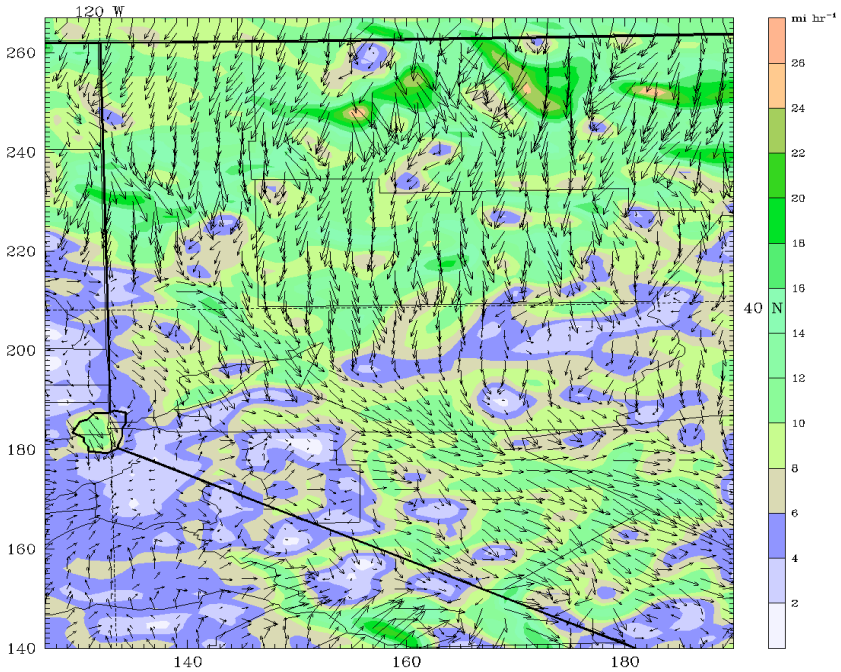

Figure 15. Zoom-in part of Domain 3 (4 km) MM5 output initialized with only ETA first guess depicting surface (~10 m) horizontal wind vectors (vectors) and horizontal wind speed (color shading) on 4 January 2005 at 0000 UTC (3 January 2005 at 1600 PST) 36 h after model initialization. Full barb = 10 mi hr^{-1} (= ~4.5 m s^{-1}).

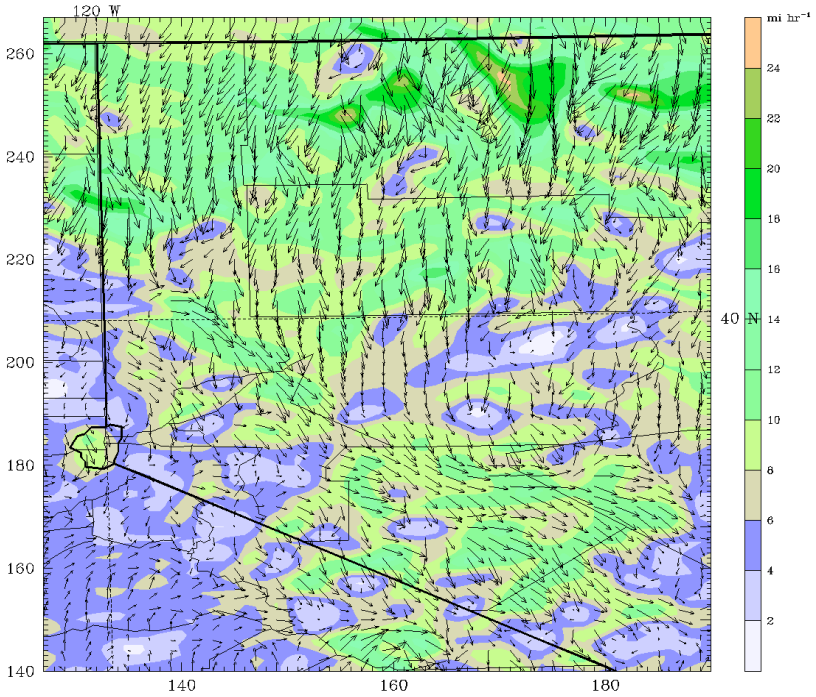

Figure 16. Zoom-in part of Domain 3 (4 km) MM5 output initialized with 3DVAR system depicting surface (~10 m) horizontal wind vectors (vectors) and horizontal wind speed (color shading) on 5 January 2005 at 0000 UTC (4 January 2005 at 1600 PST) 36 h after model initialization. Coordinates are horizontal domain grid points. Full barb = 10 mi hr^{-1} (= ~4.5 m s^{-1}).

6. CONCLUSION

WindSat data were used to prepare a 3DVAR system for initializing MM5 model. The 3DVAR observation pre-processor was modified to ingest WindSat data (along with its observation error statistics), and a QuicScat operator (an operator used in 3DVAR code to deal with the wind vector data from quick scatterometer very much similar to the new WindSat introduced in this project) was cloned to create a WindSat operator to work with the maritime wind vectors. The 3D-VAR code was run to test for the real-time statistical analysis using the initial analysis time of 3 January 2005 at 1200 UTC, and results showed reasonable diagnostic increments (positive and negative values) over the model domains.

The MM5 model was run with and without 3DVAR initializations inputs, and results were qualitatively compared to each other to assess the impact of WindSat assimilation into 3DVAR system. In general, the initialization of MM5 model by 3DVAR has produced decrease of wind speeds in most of the model domains and slight changes in wind direction in particular areas such as the foothills of the eastern Sierras. It is expected that the 3DVAR system in a cycling mode can improve the model analysis and weather prediction with the use of local meteorological observations and WindSat data, which is a task intended for the near future.

The preliminary qualitative evaluation of the wind fields with and without a 3DVAR analysis initialization indicated a better resolution with lower magnitudes in the wind fields predicted by 3DVAR-MM5; however, a complete evaluation of the implemented methods is an ongoing study that will reveal the potential influence of using WindSat winds in the 3DVAR system on the overall real-time forecasts.

REFERENCES

Arakawa, A., and V. R. Lamb, 1977: Computational design of the basic dynamical processes of the UCLA general circulation model. *Methods Comput. Phys.*, **17**, 173-265.

Barker, D. M., W. Huang, Y.-R. Guo, and A. J. Bourgeois, 2003: A Three-Dimensional Variational (3DVAR) Data Assimilation System for use with MM5. NCAR Tech. Note NCAR/TN 543 + STR, 73 pp. [Available online at: http://www.mmm.ucar.edu/individual/guo/3dvar_tutorial.htm].

Barker, D. M., W. Huang, Y.-R. Guo, A. J. Bourgeois, and Q. N. Xiao, 2004: A Three-Dimensional Data Assimilation System for MM5: Implementation and initial results. *Mon. Wea. Rev.*, **132**, 897-914.

Courtier, P., J. N. Thepaut, and A. Hollingsworth, 1994: A strategy for operational implementation of 4D-Var using an incremental app-roach. *Quart. J. Roy. Meteor. Soc.*, **120**, 1367-1387.

Dudhia, J., 1993: A Nonhydrostatic Version of the Penn State–NCAR Mesoscale Model: Validation tests and simulation of an Atlantic cyclone and cold front. *Mon. Wea. Rev.*, **121**, 1493–1513.

Grell, G., J. Dudhia, and D. Stauffer, 1994: A description of the Fifth-Generation Penn State-/NCAR Mesoscale Model (MM5). NCAR-/TN-398+STR, 117 pp. [Available online at: http://www.mmm.ucar.edu/mm5/doc1.html].

Guo, Y.-R., Y.-H. Kuo, J. Dudhia, and D. Parsons, 2000: Four-Dimensional Variational Data Assimilation of heterogeneous mesoscale observations for a strong convective case. *Mon. Wea. Rev.*, **128**, 619-643.

Janjic, Zavisa I., 1994: The step-mountain eta coordinate model: Further development of the convection, viscous sublayer, and turbulent closure schemes. Mon. Wea. Rev., **122**, 927-945.

Lorenc, A. C., and Coauthors, 2000: The Met. Office global three-dimensional variational data assimilation scheme. *Quart. J. Roy. Meteor. Soc.*, **126**, 2991-3012.

Lungu, T., 2005: WindSat science data products user's manual. Sensor and environmental data records Tech. note. Version 2.0, 46 pp. [Available online at: http:// http://-podaac.jpl.nasa.gov/index.html].

Parrish, D. F., and J. Derber, 1992: The National Meteorological Center's spectral statistical interpolation analysis system. *Mon. Wea. Rev.*, **120**, 1747-1763.

Stoelinga, M. T., 1991: A program for visualizing mesoscale model output. [Available one-line at: http://www.mmm.ucar.edu/mm5/documents/ripu g_V4.html].